leech *Hirudo medicinalis*, characterization, and sequence analysis. *Biol. Chem. Hoppe-Seyler* **375,** 685–694 (1994).
11. Stubbs, M. T. *et al.* The three dimensional structure of recombinant leech-derived tryptase inhibitor in complex with trypsin: implications for the structure of human mast cell tryptase and its inhibition. *J. Biol. Chem.* **272,** 19931–19937 (1997).
12. Kam, C. M. *et al.* Mammalian tissue trypsin-like enzymes: substrate specificity and inhibitory potency of substituted isocoumarin mechanism-based inhibitors, benzamidine derivatives, and arginine fluoroalkyl ketone transition-state inhibitors. *Arch. Biochem. Biophys.* **316,** 808–814 (1995).
13. Clark, J. M., Moore, W. R. & Tanaka, R. D. Tryptase inhibitors: a new class of antiinflammatory drugs. *Drugs Future* **21,** 811–816 (1996).
14. Johnson, D. A. & Barton, G. J. Mast cell tryptases: examination of unusual characteristics by multiple sequence alignment and molecular modeling. *Protein Sci.* **1,** 370–377 (1992).
15. Matsumoto, R., Sali, A., Ghildyal, N., Karplus, M. & Stevens, R. L. Packaging of proteases and proteoglycans in the granules of mast cells and other hematopoietic cells. A cluster of histidines on mouse mast cell protease 7 regulates its binding to heparin serglycin proteoglycans. *J. Biol. Chem.* **270,** 19524–19531 (1995).
16. Fujinaga, M., Chernaia, M. M., Halenbeck, R., Koths, K. & James, M. N. The crystal structure of PR3, a neutrophil serine proteinase antigen of Wegener's granulomatosis antibodies. *J. Mol. Biol.* **261,** 267–278 (1996).
17. Bode, W. & Schwager, P. The refined crystal structure of bovine beta-trypsin at 1.8 Å resolution. II. Crystallographic refinement, calcium binding site, benzamidine binding site and active site at pH 7.0. *J. Mol. Biol.* **98,** 693–717 (1975).
18. Walter, J. & Bode, W. The X-ray crystal structure analysis of the refined complex formed by bovine trypsin and p-amidinophenylpyruvate at 1.4 Å resolution. *Hoppe-Seyler's Z. Physiol. Chem.* **364,** 949–959 (1983).
19. Stürzebecher, J., Prasa, D. & Sommerhoff, C. P. Inhibition of human mast cell tryptase by benzamidine derivatives. *Biol. Chem. Hoppe-Seyler* **373,** 1025–1030 (1992).
20. Caughey, G. H., Raymond, W. W., Bacci, E., Lombardy, R. J. & Tidwell, R. R. Bis(5-amidino-2-benzimidazolyl)methane and related amidines are potent, reversible inhibitors of mast cell tryptases. *J. Pharmacol. Exp. Ther.* **264,** 676–682 (1993).
21. Fiorucci, L., Erba, F., Bolognesi, M., Coletta, M. & Ascoli, F. pH dependence of bovine mast cell tryptase catalytic activity and of its inhibition by 4′,6-diamidino-2-phenylindole. *FEBS Lett.* **408,** 85–88 (1997).
22. Bode, W. & Huber, R. Natural protein proteinase inhibitors and their interaction with proteinases. *Eur. J. Biochem.* **204,** 433–451 (1992).
23. Otwinowski, Z. & Minor, W. *DENZO: a Film Processing for Macromolecular Crystallography* (Yale Univ., 1993).
24. Navaza, J. An automated package for molecular replacement. *Acta Crystallogr. A* **50,** 157–163 (1994).
25. Roussel, A. & Cambilleau, C. *TurboFRODO in Sillicon Graphics Geometry* (Sillicon Graphics, Mountain View, California, 1989).
26. Collaborative Computational Project No. 4. The CCP4 suite: programs for protein crystallography. *Acta Crystallogr. D* **50,** 760–763 (1994).
27. Brünger, G. J. *XPLOR (version 3.1). A System for X-ray Crystallography and NMR* (Yale Univ. Press, 1993).
28. Nicholls, A., Bharadwaj, R. & Honig, B. GRASP—graphical representation and analysis of surface properties. *Biophys. J.* **64,** A166 (1993).
29. Barton, G. J. ALSCRIPT: a tool to format multiple sequence alignments. *Protein Eng.* **6,** 37–40 (1993).
30. Evans, S. V. SETOR: hardware lighted three-dimensional solid model representations of macromolecules. *J. Mol. Graph.* **11,** 134–138 (1990).

Acknowledgements. We thank D. Grosse for help in protein crystallization, R. Mentele for amino-acid-sequence analysis, and M. T. Stubbs for reading the paper. This work was supported by scholarships from Programa Praxis XXI of the Fundação para a Ciência e a Tecnologia and the Programa Gulbenkian de Doutoramento em Biologia e Medicina, Portugal, and by Biotech programs of the European Union, the Sonderforschungsbereich 469 of the University of Munich, the Deutsche Forschungsgemeinschaft and the Fonds der Chemischen Industrie.

Correspondence and requests for materials should be addressed to W.B. (e-mail: bode@biochem.mpg.de). The coordinates have been deposited with the Brookhaven Protein Data Bank under accession number 1A0L.

erratum

Discovery of a supernova explosion at half the age of the Universe

S. Perlmutter[1,2], G. Aldering[1], M. Della Valle[3], S. Deustua[1,4], R. S. Ellis[5], S. Fabbro[1,6,7], A. Fruchter[8], G. Goldhaber[1,2], A. Goobar[9], D. E. Groom[1], I. M. Hook[1,10], A. G. Kim[1,11], M. Y. Kim[1], R. A. Knop[1], C. Lidman[12], R. G. McMahon[5], P. Nugent[1], R. Pain[1,6], N. Panagia[13], C. R. Pennypacker[1,4], P. Ruiz-Lapuente[14], B. Schaefer[15] & N. Walton[16]

Nature **391,** 51–54 (1998)

The name of one of the authors (Ariel Goobar) of this Letter was inadvertently removed during page make-up. A. Goobar is in the Physics Department, Stockholm University, as indicated in the footnote addresses. □

retracted correction

CTL induction by a tumour-associated antigen octapeptide derived from a murine lung carcinoma

Ofer Mandelboim, Gideon Berke, Mati Fridkin, Michael Feldman, Miriam Eisenstein & Lea Eisenbach

Nature **369,** 67–71 (1994)

A Correction to this Letter was published on 11 December 1997 (*Nature* **390,** 643; 1997), submitted by one of the authors (G.B.). However, because of an error in the editorial office, the correction had bypassed our standard procedures of checking with all authors and, where differences arise, with peer reviewers. The Correction therefore should not have been published. It has since become clear that the matter is one of scientific disagreement between G.B. and the other authors, who stand by their results in the original paper. □

Discovery of a supernova explosion at half the age of the Universe

S. Perlmutter[1,2], G. Aldering[1], M. Della Valle[3], S. Deustua[1,4], R. S. Ellis[5], S. Fabbro[1,6,7], A. Fruchter[8], G. Goldhaber[1,2], D. E. Groom[1], I. M. Hook[1,10], A. G. Kim[1,11], M. Y. Kim[1], R. A. Knop[1], C. Lidman[12], R. G. McMahon[5], P. Nugent[1], R. Pain[1,6], N. Panagia[13], C. R. Pennypacker[1,4], P. Ruiz-Lapuente[14], B. Schaefer[15] & N. Walton[16]

The ultimate fate of the Universe, infinite expansion or a big crunch, can be determined by using the redshifts and distances of very distant supernovae to monitor changes in the expansion rate. We can now find[1] large numbers of these distant supernovae, and measure their redshifts and apparent brightnesses; moreover, recent studies of nearby type Ia supernovae have shown how to determine their intrinsic luminosities[2–4]—and therefore with their apparent brightnesses obtain their distances. The >50 distant supernovae discovered so far provide a record of changes in the expansion rate over the past several billion years[5–7]. However, it is necessary to extend this expansion history still farther away (hence further back in time) in order to begin to distinguish the causes of the expansion-rate changes—such as the slowing caused by the gravitational attraction of the Universe's mass density, and the possibly counteracting effect of the cosmological constant[8]. Here we report the most distant spectroscopically confirmed supernova. Spectra and photometry from the largest telescopes on the ground and in space show that this ancient supernova is strikingly similar to nearby, recent type Ia supernovae. When combined with previous measurements of nearer supernovae[2,5], these new measurements suggest that we may live in a low-mass-density universe.

SN1997ap was discovered by the Supernova Cosmology Project collaboration on 5 March 1997 UT, during a two-night search at the Cerro Tololo Interamerican Observatory (CTIO) 4-m telescope that yielded 16 new supernovae. The search technique finds such sets of high-redshift supernovae on the rising part of their light curves and guarantees the date of discovery, thus allowing follow-up photometry and spectroscopy of the transient supernovae to be scheduled[1]. The supernova light curves were followed with scheduled R-, I- and some B-band photometry at the CTIO, WIYN, ESO 3.6-m, and INT telescopes, and with spectroscopy at the ESO 3.6-m and Keck II telescopes. (Here WIYN is the Wisconsin, Indiana, Yale, NOAO Telescope, ESO is the European Southern Observatory, and INT is the Isaac Newton Telescope.) In addition, SN1997ap was followed with scheduled photometry on the Hubble Space Telescope (HST).

Figure 1 shows the spectrum of SN1997ap, obtained on 14 March 1997 UT with a 1.5-h integration on the Keck II 10-m telescope. There is negligible (≤5%) host-galaxy light contaminating the supernova spectrum, as measured from the ground- and space-based images. When fitted to a time series of well-measured nearby type Ia supernova spectra[9], the spectrum of SN1997ap is most consistent with a 'normal' type Ia supernova at redshift $z = 0.83$ observed 2 ± 2 supernova-restframe days (~4 observer's days) before the supernova's maximum light in the rest-frame B band. It is a poor match to the 'abnormal' type Ia supernovae, such as the brighter SN1991T or the fainter SN1986G. For comparison, the spectra of low-redshift, 'normal' type Ia supernovae are shown in Fig. 1 with wavelengths redshifted as they would appear at $z = 0.83$. These spectra show the time evolution from 7 days before, to 2 days after, maximum light.

Figure 2 shows the photometry data for SN1997ap, with significantly smaller error bars for the HST observations (Fig. 2a) than for the ground-based observations (Fig. 2b and c). The width of the light curve of a type Ia supernova has been shown to be an excellent indicator of its intrinsic luminosity, both at low redshift[2–4] and at high redshift[5]: the broader and slower the light curve, the brighter

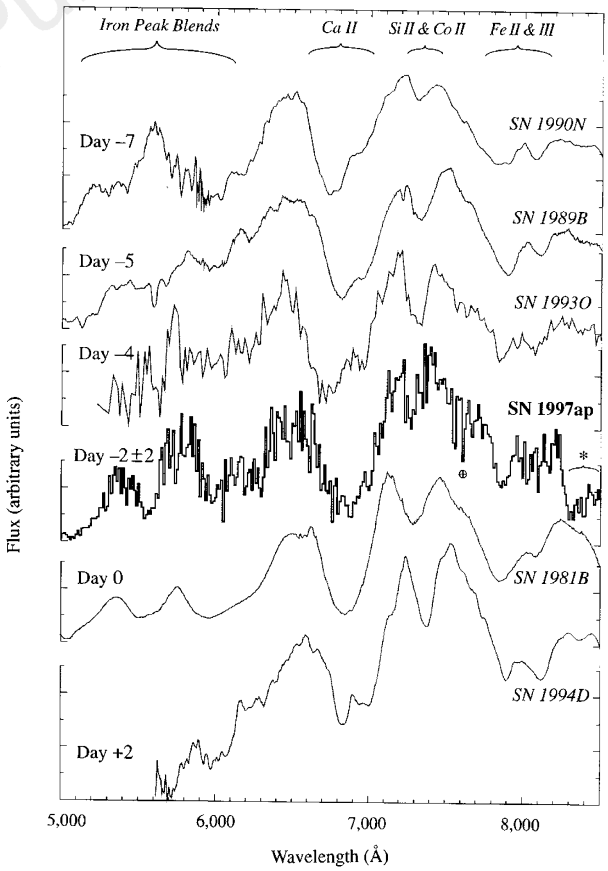

Figure 1 Spectrum of SN1997ap placed within a time sequence of five 'normal' type Ia supernovae. The data for SN1997ap have been binned by 12.5 Å; the time series of spectra of the other supernovae[17–21] (the spectrum of SN1993O was provided courtesy of the Calán/Tololo Supernova Survey) are given as they would appear redshifted to $z = 0.83$. The spectra show the evolution of spectral features between 7 rest-frame days before, and 2 days after, rest-frame B-band maximum light. SN1997ap matches best at 2 ± 2 days before maximum light. The symbol ⊕ indicates an atmospheric absorption line and * indicates a region affected by night-sky line subtraction residuals. The redshift of $z = 0.83 \pm 0.005$ was determined from the supernova spectrum itself, as there were no host galaxy lines detected.

[1] E. O. Lawrence Berkeley National Laboratory, 1 Cyclotron Road, MS 50-232, Berkeley, California 94720, USA. [2] Center for Particle Astrophysics, University of California, Berkeley, California 94720, USA. [3] Dipartimento di Astronomia, Universita' di Padova, Vicolo Osservatorio 5, 35122, Padova, Italy. [4] Space Sciences Laboratory, University of California, Berkeley, California 94720, USA. [5] Institute of Astronomy, Madingley Road, Cambridge CB3 0HA, UK. [6] LPNHE, Universites Paris VI & VII, T33 Rdc, 4, Place Jussieu, 75252 Paris Cedex 05, France. [7] Observatoire de Strasbourg, 11, Rue de l'Universite, 67000 Strasbourg, France. [8] Space Telescope Science Institute, 3700 San Martin Drive, Baltimore, Maryland 21218, USA. [9] Physics Department, Stockholm University, Box 6730, S-11385 Stockholm, Sweden. [10] European Souther Observatory, Karl-Schwarzschild-Strasse 2, D-85748 Garching bei Munchen, Germany. [11] Physique Corpusculaire et Cosmologie, Collège de France, 11, Place Marcelin-Berthelot, 75231 Paris, France. [12] European Southern Observatory, Alonso de Cordova, 3107, Vitacura, Casilla 19001, Santiago, 19, Chile. [13] Space Telescope Science Institute, 3700 San Martin Drive, Baltimore, Maryland 21218, USA; affiliated with the Astrophysics Division, Space Science Department of ESA. [14] Department of Astronomy, Faculty of Physics, University of Barcelona, Diagonal 647, E-08028 Barcelona, Spain. [15] Department of Physics, Yale University, 260 Whitney Avenue, JWG 463, New Haven, Connecticut 06520, USA. [16] Isaac Newton Group, Apartado 321, 38780 Santa Cruz de La Palma, The Canary Islands, Spain.

the supernova is at maximum. We characterize this width by fitting the photometry data to a 'normal' type Ia supernova template light curve that has its time axis stretched or compressed by a linear factor, called the 'stretch factor'[1,5]; a 'normal' supernova such as SN1989B, SN1993O or SN1981B in Fig. 1 thus has a stretch factor of $s \approx 1$. To fit the photometry data for SN1997ap, we use template U- and B-band light curves that have first been $1 + z$ time-dilated and wavelength-shifted ('*K*-corrected') to the R- and I-bands as they would appear at $z = 0.83$ (see ref. 5 and P.N. *et al.*, manuscript in preparation). The best-fit stretch factor for all the photometry of Fig. 2 indicates that SN1997ap is a 'normal' type Ia supernova: $s = 1.03 \pm 0.05$ when fitted for a date of maximum at 16.3 March 1997 UT (the error-weighted average of the best-fit dates from the light curve, 15.3 ± 1.6 March 1997 UT, and from the spectrum, 18 ± 3 March 1997 UT).

It is interesting to note that we could alternatively fit the $1 + z$ time dilation of the event while holding the stretch factor constant at $s = 1.0^{+0.05}_{-0.14}$ (the best fit value from the spectral features obtained in ref. 10). We find that the event lasted $1 + z = 1.86^{+0.31}_{-0.09}$ times longer than a nearby $s = 1$ supernova, providing the strongest confirmation yet of the cosmological nature of redshift[9,11,12].

The best-fit peak magnitudes for SN1997ap are $I = 23.20 \pm 0.07$ and $R = 24.10 \pm 0.09$. (All magnitudes quoted or plotted here are transformed to the standard Cousins[13] R and I bands.) These peak magnitudes are relatively insensitive to the details of the fit: if the date of maximum is left unconstrained or set to the date indicated by the best-match spectrum, or if the ground- and space-based data are fitted alone, the peak magnitudes still agree well within errors.

The ground-based data show no evidence of host-galaxy light, but the higher-resolution HST imaging shows a marginal detection (after co-adding all four dates of observation) of a possible $I = 25.2 \pm 0.3$ host galaxy 1 arcsec from the supernova. This light does not contaminate the supernova photometry from the HST and it contributes negligibly to the ground-based photometry. The projected separation is ~6 kpc (for $\Omega_M = 1$, $\Omega_\Lambda = 0$ and $h_0 = 0.65$, the dimensionless cosmological parameters describing the mass density, vacuum energy density and Hubble constant, respectively) and the corresponding *B*-band rest-frame magnitude is $M_B \approx -17$ and its surface brightness is $\mu_B \approx 21$ mag arcsec^{-2}, consistent with properties of local spiral galaxies. We note that the analysis will need a final measurement of any host-galaxy light after the supernova has faded, in the unlikely event that there is a very small knot of host-galaxy light directly under the HST image of SN1997ap.

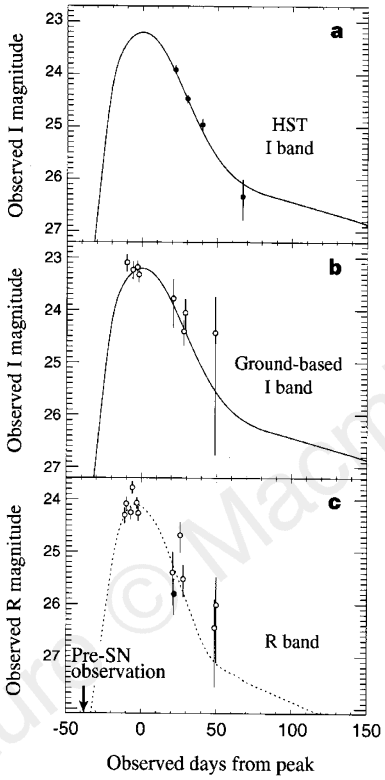

Figure 2 Photometry points for SN1997ap. **a**, As observed by the HST in the F814W filter; **b** as observed with ground-based telescopes in the Harris I filter; and **c**, as observed with the ground-based telescopes in the Harris R filter (open circles) and the HST in the F675W filter (filled circle); with all magnitudes corrected to the Cousins I or R systems[13]. The solid line shown in both **a** and **b** is the simultaneous best fit to the ground- and space-based data to the *K*-corrected, $(1+z)$ time-dilated Leibundgut B-band type Ia supernova template light curve[22], and the dotted line in **c** is the best fit to a *K*-corrected, time-dilated U-band type Ia supernova template light curve. The ground-based data was reduced and calibrated following the techniques of ref. 5, but with no host-galaxy light subtraction necessary. The HST data was calibrated and corrected for charge-transfer inefficiency following the prescriptions of refs 23, 24. *K*-corrections were calculated as in ref. 25, modified for the HST filter system. Correlated zero-point errors are accounted for in the simultaneous fit of the light curve. The errors in the calibration, charge-transfer inefficiency correction and *K*-corrections for the HST data are much smaller (~4% total) than the contributions from the photon noise. No corrections were applied to the HST data for a possible ~4% error in the zero points (P. Stetson, personal communication) or for nonlinearities in the WFPC2 response[26], which might bring the faintest of the HST points into tighter correspondence with the best-fit light curve in **a** and **c**. Note that the individual fits to the data in **a** and **b** agree within their error bars, providing a first-order cross-check of the HST calibration.

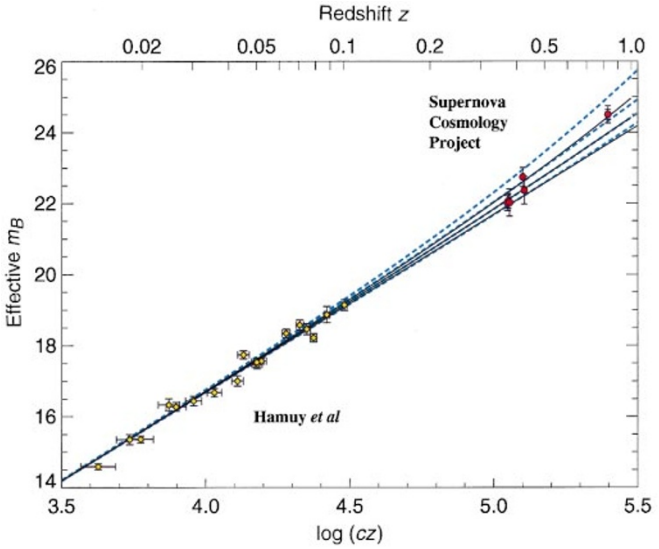

Figure 3 SN1997ap at $z = 0.83$ plotted on the Hubble diagram from ref. 5. Also plotted are the 5 of the first 7 high-redshift supernovae that could be width-luminosity corrected, and the 18 of the lower-redshift supernovae from the Calán/Tololo Supernova Survey that were observed earlier then 5 d after maximum light[3]. Magnitudes have been *K*-corrected, and also corrected for the width-luminosity relation. The inner error bar on the SN1997ap point corresponds to the photometry error alone, while the outer error bar includes the intrinsic dispersion of type Ia supernovae after stretch correction (see text). The solid curves are theoretical m_B for $(\Omega_M, \Omega_\Lambda) = (0,0)$ on top, $(1,0)$ in middle and $(2,0)$ on bottom. The dotted curves are for the flat-universe case, with $(\Omega_M, \Omega_\Lambda) = (0,1)$ on top, $(0.5, 0.5)$, $(1,0)$ and $(1.5, -0.5)$ on bottom.

We compare the K-corrected R–I observed difference of peak magnitudes (measured at the peak of each band, not the same day) to the U–B colour found for 'normal' low-redshift type Ia supernovae. We find that the rest-frame colour of SN1997ap $[(U-B)_{\mathrm{SN1997ap}} = -0.28 \pm 0.11]$ is consistent with an unreddened 'normal' type Ia supernova colour, $(U-B)_{\mathrm{normal}} = -0.32 \pm 0.12$ (see ref. 14 and also P.N. *et al.*, manuscript in preparation). In this region of the sky, there is also no evidence for Galactic reddening[15]. Given the considerable projected distance from the putative host galaxy, the supernova colour, and the lack of galaxy contamination in the supernova spectra, we proceed with an analysis under the hypothesis that the supernova suffers negligible host-galaxy extinction, but with the following caveat.

Although correcting for $E(U-B) \approx 0.04$ of reddening would shift the magnitude by only one standard deviation, $A_B = 4.8E(U-B) = 0.19 \pm 0.78$, the uncertainty in this correction would then be the most significant source of uncertainty for this one supernova. This is because of the large uncertainty in the $(U-B)_{\mathrm{SN1997ap}}$ measurement, and the sparse low-redshift U-band reference data. HST J-band observations are currently planned for future $z > 0.8$ supernovae, to allow a comparison with the restframe $B-V$ colour, a much better indicator of reddening for type Ia supernovae. Such data will thus provide an important improvement in extinction correction uncertainties for future supernovae and eliminate the need for assumptions regarding host-galaxy extinction. In the following analysis, we also do not correct the lower-redshift supernovae for possible host-galaxy extinction, so any similar distribution of extinction would partly compensate for this possible bias in the cosmological measurements.

The significance of type Ia supernovae at $z = 0.83$ for measurements of the cosmological parameters is illustrated on the Hubble diagram of Fig. 3. To compare with low-redshift magnitudes, we plot SN1997ap at an effective rest-frame B-band magnitude of $B = 24.50 \pm 0.15$, derived, as in ref. 5, by adding a K-correction and increasing the error bar by the uncertainty due to the (small) width-luminosity correction and by the intrinsic dispersion remaining after this correction. By studying type Ia supernovae at twice the redshift of our first previous sample at $z \approx 0.4$, we can look for a correspondingly larger magnitude difference between the cosmologies considered. At the redshift of SN1997ap, a flat $\Omega_M = 1$ universe is separated from a flat $\Omega_M = 0.1$ universe by almost one magnitude, as opposed to half a magnitude at $z \approx 0.4$. For comparison, the uncertainty in the peak magnitude of SN1997ap is only 0.15 mag, while the intrinsic dispersion amongst stretch-calibrated type Ia supernovae is ~0.17 mag (ref. 5). Thus, at such redshifts even individual type Ia supernovae become powerful tools for discriminating amongst various world models, provided observations are obtained, such as those presented here, where the photometric errors are below the intrinsic dispersion of type Ia supernova.

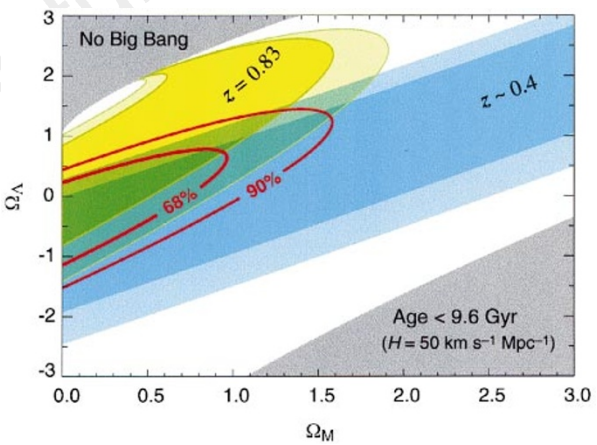

Figure 4 Contour plot of the best fit confidence regions in the Ω_Λ versus Ω_M plane for SN1997ap and the five supernovae at $z \approx 0.4$ (see ref. 5). The 68% (1σ) and 90% confidence regions for (blue shading) the supernovae at $\zeta \approx 0.4$, (yellow shading) SN1997ap at $z = 0.83$ by itself, and (red contours) all of these supernovae taken together. The two labelled corners of the plot are ruled out because they imply: (upper left corner) a 'bouncing' universe with no Big Bang[27], or (lower right corner) a universe younger than the oldest heavy elements, $t_0 < 9.6$ Gyr (ref. 28), for any value of $H_0 \geq 50$ km s^{-1} Mpc^{-1}.

By combining such data spanning a large range of redshift, it is also possible to distinguish between the effects of mass density Ω_M and cosmological constant Λ on the Hubble diagram[8]. The blue contours of Fig. 4 show the allowed confidence region on the Ω_Λ ($\equiv \Lambda/(3H_0^2)$) versus Ω_M plane for the $z \approx 0.4$ supernovae[5]. The yellow contours show the confidence region from SN1997ap by itself, demonstrating the change in slope of the confidence region at higher redshift. The red contours show the result of the combined fit, which yields a closed confidence region in the Ω_M–Ω_Λ plane. This fit corresponds to a value of $\Omega_M = 0.6 \pm 0.2$ if we constrain the result to a flat universe ($\Omega_\Lambda + \Omega_M = 1$), or $\Omega_M = 0.2 \pm 0.4$ if we constrain the result to a $\Lambda = 0$ universe. These results are preliminary evidence for a relatively low-mass-density universe. The addition of SN1997ap to the previous sample of lower-redshift supernovae decreases the best-fit Ω_M by approximately 1 standard deviation compared to the earlier results[5].

Our data for SN1997ap demonstrate: (1) that type Ia supernovae at $z > 0.8$ exist; (2) that they can be compared spectroscopically with nearby supernovae to determine supernova ages and luminosities and check for indications of supernova evolution; and (3) that calibrated peak magnitudes with precision better than the intrinsic dispersion of type Ia supernovae can be obtained at these high redshifts. The width of the confidence regions in Fig. 4 and the size of the corresponding projected measurement uncertainties show that with additional type Ia supernovae having data of quality comparable to that of SN1997ap, a simultaneous measurement of Ω_Λ and Ω_M is now possible. It is important to note that this measurement is based on only one supernova at the highest ($z > 0.8$) redshifts, and that a larger sample size is required to find a statistical peak and identify any 'outliers'. In particular, SN1997ap was discovered near the search detection threshold and thus may be drawn from the brighter tail of a distribution ('Malmquist bias'). There is similar potential bias in the lower-redshift supernovae of the Calán/Tololo Survey[2], making it unclear which direction such a bias would change Ω_M.

Several more supernovae at comparably high redshift have already been discovered by the Supernova Cosmology Project collaboration, including SN1996cl, also at $z = 0.83$. SN1996cl can be identified as a very probable type Ia supernova, as a serendipitous HST observation (M. Donahue *et al.*, personal communication) shows its host galaxy to be an elliptical or S0. Its magnitude and colour, although much more poorly constrained by photometry data, agree within uncertainty with those of SN1997ap. The next most distant spectroscopically confirmed type Ia supernovae are at $z = 0.75$ and $z = 0.73$ (ref. 16; these supernovae are awaiting final calibration data). In the redshift range $z = 0.3$–0.7, we have discovered over 30 additional spectroscopically confirmed type Ia supernovae, and followed them with two-filter photometry. (The first sample of supernovae with $z \approx 0.4$ were not all spectroscopically confirmed and observed with two-filter photometry[5].) These new supernovae will improve both the statistical and systematic uncertainties in our measurement of Ω_M and Ω_Λ in combination. A matching sample of ≥ 6 type Ia supernovae at $z > 0.7$ is to be observed in two filters in Hubble Space Telescope observations due to start on 5 January 1998. SN1997ap demonstrates the efficacy of these complementary higher-redshift measurements in separating

the contribution of Ω_M and Ω_Λ to the total mass-energy density of the Universe.

Received 7 October; accepted 18 November 1997.

1. Perlmutter, S. *et al.* in *Thermonuclear Supernovae* (eds Ruiz-Lapuente, P. *et al.*) 749–763 (Kluwer, Dordrecht, 1997).
2. Phillips, M. M. The absolute magnitudes of Type Ia supernovae. *Astrophys. J.* **413,** L105–L108 (1993).
3. Hamuy, M. *et al.* The absolute luminosities of the Calán/Tololo Type Ia supernovae. *Astron. J.* **112,** 2391–2397 (1996).
4. Riess, A. G., Press, W. H. & Kirshner, R. P. Using Type Ia supernova light curve shapes to measure the Hubble constant. *Astrophys. J.* **438,** L17–L20 (1995).
5. Perlmutter, S. *et al.* Measurements of the cosmological parameters Ω and Λ from the first seven supernovae at $z \geq 0.35$. *Astrophys. J.* **483,** 565–581 (1997).
6. Perlmutter, S. *et al. IAU Circ.* No. 6621 (1997).
7. Schmidt, B. *et al. IAU Circ.* No. 6646 (1997).
8. Goobar, A. & Perlmutter, S. Feasibility of measuring the cosmological constant Λ and mass density Ω using Type Ia supernovae. *Astrophys. J.* **450,** 14–18 (1995).
9. Riess, A. G. *et al.* Time dilation from spectral feature age measurements of Type Ia supernovae. *Astron. J.* **114,** 722–729 (1997).
10. Nugent, P. *et al.* Evidence for a spectroscopic sequence among Type Ia supernovae. *Astrophys. J.* **455,** L147–L150 (1993).
11. Goldhaber, G. *et al.* in *Thermonuclear Supernovae* (eds Ruiz-Lapuente, P. *et al.*) 777–784 (Kluwer, Dordrecht, 1997).
12. Leibundgut, B. *et al.* Time dilation in the light curve of the distant Type Ia supernova SN 1995K. *Astrophys. J.* **466,** L21–L44 (1996).
13. Bessell, M. S. UBVRI passbands. *Publ. Astron. Soc. Pacif.* **102,** 1181–1199 (1990).
14. Branch, D., Nugent, P. & Fisher, A. in *Thermonuclear Supernovae* (eds Ruiz-Lapuente, P. *et al.*) 715–734 (Kluwer, Dordrecht, 1997).
15. Burstein, D. & Heiles, C. Reddenings derived from H I and galaxy counts—accuracy and maps. *Astron. J.* **87,** 1165–1189 (1982).
16. Perlmutter, S. *et al. IAU Circ.* No. 6540 (1997).
17. Leibundgut, B. *et al.* Premaximum observations of the type Ia SN 1990N. *Astrophys. J.* **371,** L23–L26 (1991).
18. Wells, L. A. *et al.* The type Ia supernova 1989B in NGC 3627 (M66). *Astron. J.* **108,** 2233–2250 (1994).
19. Branch, D. *et al.* The type I supernova 1981b in NGC 4536: the first 100 days. *Astrophys. J.* **270,** 123–139 (1983).
20. Patat, F. *et al.* The Type Ia supernova 1994D in NGC 4526: the early phases. *Mon. Not. R. Astron. Soc.* **278,** 111–124 (1996).
21. Cappellaro, E., Turatto, M. & Fernley, J. in *IUE—ULDA Access Guide No. 6: Supernovae* (eds Cappellaro, E., Turatto, M. & Fernley, J.) 1–180 (ESA, Noordwijk, 1995).
22. Leibundgut, B., Tammann, G., Cadonau, R. & Cerrito, D. Supernova studies. VII. An atlas of light curves of supernovae type I. *Astron. Astrophys. Suppl. Ser.* **89,** 537–579 (1991).
23. Holtzman, J. *et al.* The photometric performance and calibration of WFPC2. *Publ. Astron. Soc. Pacif.* **107,** 1065–1093 (1995).
24. Whitmore, B. & Heyer, I. *New Results on Charge Transfer Efficiency and Constraints on Flat-Field Accuracy* (Instrument Sci. Rep. WFPC2 97-08, Space Telescope Science Institute, Baltimore, 1997).
25. Kim, A., Goobar, A. & Perlmutter, S. A generalized K-corrections for Type Ia supernovae: comparing R-band photometry beyond z = 0.2 with B, V, and R-band nearby photometry. *Publ. Astron. Soc. Pacif.* **108,** 190–201 (1996).
26. Stiavelli, M. & Mutchler, M. *WFPC2 Electronics Verification* (Instrument Sci. Rep. WFPC2 97-07, Space Telescope Science Institute, Baltimore, 1997).
27. Carrol, S., Press, W. & Turner, E. The cosmological constant. *Annu. Rev. Astron. Astrophys.* **30,** 499–542 (1992).
28. Schramm, D. in *Astrophysical Ages and Dating Methods* (eds Vangioni-Flam, E. *et al.*) 365–384 (Editions Frontières, Gif sur Yvette, 1990).

Acknowledgements. The authors are members of the Supernova Cosmology Project. We thank CTIO, Keck, HST, WIYN, ESO and the ORM–La Palma observatories for a generous allocation of time, and the support of dedicated staff in pursuit of this project; D. Harmer, P. Smith and D. Willmarth for their help as WIYN queue observers; and G. Bernstein and A. Tyson for developing and supporting the Big Throughput Camera which was instrumental in the discovery of this supernova.

Correspondence and requests for materials should be addressed to S.P. (e-mail: saul@lbl.gov).

The inner edge of the accretion disk around a supermassive black hole

B. C. Bromley*, W. A. Miller† & V. I. Pariev†‡

* *Theoretical Astrophysics, Harvard-Smithsonian Center for Astrophysics, MS-51, 60 Garden Street, Cambridge, Massachusetts 02138, USA*
† *Theoretical Astrophysics, MS B288, Los Alamos National Laboratory, Los Alamos, New Mexico 87545, USA*
‡ *P. N. Lebedev Physical Institute, Leninsky Prospect 53, Moscow 117924, Russia*

Massive black holes are generally thought to exist at the centres of galaxies[1], but an unambiguous identification of a black hole has been impeded by a lack of evidence for the strong-field relativistic effects expected in the vicinity of such an object. Several years ago, a very broad iron emission line was discovered in the active galaxy MCG-6-30-15, indicative of emission from an accretion disk near the event horizon of a black hole. But this interpretation, based on the line profile, was somewhat model dependent (refs 2–5). Here we present an analysis of the iron-line emission from MCG-6-30-15 that is insensitive to the details (for example, disk thickness and emissivity) of the disk model used. We find that the inner edge of the disk material giving rise to the line is within 2.6 ± 0.3 times the Schwarzschild radius—the event horizon of a non-rotating black hole—at the 95% confidence level. Changes to the disk parameters can only decrease the inner radius of the emitting region, and so we can be confident that we are observing emission from gravitationally bound material in the strong-field region of a supermassive black hole. Moreover, we find that the black hole is rotating at a rate which is $\gtrsim 23 \pm 17\%$ of the theoretical maximum, although this conclusion is model dependent.

The iron Kα line from MCG-6-30-15, produced by fluorescence in the presence of a hard X-ray source, has distinct features which are uniquely characteristic of a relativistic accretion disk. The line is peaked near the rest-frame energy of 6.4 keV, with a broad red wing possibly containing a second weaker peak, the analogue of the red horn in the double-peaked, Doppler-shifted profile of a non-relativistic keplerian disk. The red peak in the relativistic case is smoothed by the effect of strong gravitational redshift. The skewness of the profile towards the red, and the sharp blue edge near the rest-frame energy, are evidently unique to relativistic accretion disks[3]; other mechanisms of line formation, involving collimated jets, outflows, chaotic clouds, and non-disk emitters/absorbers all fail to produce these features. Thus the MCG-6-30-15 iron line is properly interpreted in the context of a relativistic disk.

This iron line, with the kinematical information it contains, offers an opportunity to firmly identify the energy source in the galactic nucleus as a supermassive black hole. A key to this identification is the size of the central object as constrained by the inner radius of disk emission. Fits to the line profile with simple disk models suggest[2,4,5] that the inner edge of the disk is within a few R_s (where $R_s \equiv 2GM/c^2$ is the Schwarzschild radius) of an object of mass M. Unfortunately, the inner radius inferred from profile fitting is subject to considerable uncertainty, partly from idealizations of the line profile models. These idealizations include a planar (zero-thickness) disk with a time-independent surface emissivity that varies only with radius. Furthermore, profile fitting requires models of the primary hard X-ray continuum, its reflection from the disk, Kα emission from species other than iron, contamination from non-disk line emitters, and absorption by intervening gas or dust. Thus it can be difficult to isolate the line emission associated with the disk.

Here we seek to constrain the inner radius of emission without an accurate assessment of the entire line profile. We take advantage of the fact that the extent of the red wing—the minimum frequency at which statistically significant line flux is observed—places a firm limit on the inner radius of the disk. Detectable flux at a particular redshift requires material to be located within some finite radius, and *all* disk models consistent with this flux must have an inner edge within this radius. Like profile fitting, measurement of the red edge of a line suffers from uncertainties in the continuum emission, which can be very problematical if the red wing has shallow fall-off (as is the case at small radii). Therefore, it is important to choose a conservative measure of the line's extent.

Our analysis is based on the extreme frequency shifts of a line profile as determined by measurable flux in both the red and blue wings. In general, the red edge of the profile comes from emission in the innermost part of the disk where gravitational redshifting is strong, and where material is flowing away from the observer, thereby inducing a Doppler redshift. The gravitational redshift is most important when the inclination angle is low, as the line-of-sight velocity component is relatively small. Within a few Schwarzschild radii, the gravitational redshift is so strong that it dominates over Doppler blueshifts, even from the most rapid line-of-sight

X-PLOR[28]. As model building and refinement progressed, the monomer mask and NCS operators were updated and unbiased experimental maps recalculated. No sigma cut was applied during refinement (Table 2). Solvent molecules were not included in the model.

Received 24 July; accepted 23 September 1997.

1. Coux, O., Tanaka, K. & Goldberg, A. L. Structure and functions of the 20S and 26S proteasomes. *Annu. Rev. Biochem.* **65,** 801–847 (1996).
2. Hoffman, L. & Rechsteiner, M. in *Current Topics in Cellular Regulation* (eds Stadtman, E. R. & Chock, P. B.) 1–32 (Academic, San Diego, 1996).
3. Peters, J.-M., Cejka, Z., Harris, J. R., Kleinschmidt, J. A. & Baumeister, W. Structural features of the 26S proteasome complex. *J. Mol. Biol.* **234,** 932–937 (1993).
4. Gray, C. W., Slaughter, C. A. & DeMartino, G. N. PA28 activator protein forms regulatory caps on proteasome stacked rings. *J. Mol. Biol.* **236,** 7–15 (1994).
5. Peters, J.-M. Proteasomes: protein degradation machines of the cell. *Trends Biochem. Sci.* **19,** 377–382 (1994).
6. Ma, C.-P., Slaughter, C. A. & DeMartino, G. N. Identification, purification and characterization of a protein activator (PA28) of the 20S proteasome (macropain). *J. Biol. Chem.* **267,** 10515–10523 (1992).
7. Dubiel, W., Pratt, G., Ferrell, K. & Rechsteiner, M. Purification of an 11S regulator of the multicatalytic protease. *J. Biol. Chem.* **267,** 22369–22377 (1992).
8. Groettrup, M. *et al.* A role for the proteasome regulator PA28α in antigen presentation. *Nature* **381,** 166–168 (1996).
9. Dick, T. P. *et al.* Coordinated dual cleavage induced by the proteasome regulator PA28 leads to dominant MHC ligands. *Cell* **86,** 253–262 (1996).
10. Ahn, J. Y. *et al.* Primary structures of two homologous subunits of PA28, a γ-interferon-inducible protein activator of the 20S proteasome. *FEBS Lett.* **366,** 37–42 (1995).
11. Realini, C. *et al.* Characterization of recombinant REGα, REGβ and REGγ proteasome activators. *J. Biol. Chem.* **272,** 25483–25492 (1997).
12. Johnston, S. C., Whitby, F. W., Realini, C., Rechsteiner, M. & Hill, C. P. The proteasome 11S regulator subunit REGα (PA28α) is a heptamer. *Prot. Sci.* **6,** 2469–2473 (1997).
13. Realini, C., Dubiel, W., Pratt, G., Ferrell, K. & Rechsteiner, M. Molecular cloning and expression of a gamma-interferon inducible activator of the multicatalytic protease. *J. Biol. Chem.* **269,** 20727–20732 (1994).
14. Ustrell, V., Realini, C., Pratt, G. & Rechsteiner, M. Human lymphoblast and erythrocyte multicatalytic proteases: differential peptidase activities and responses to the 11S regulator. *FEBS Lett.* **376,** 155–158 (1995).
15. Ahn, K. *et al. In vivo* characterization of the proteasome regulator PA28. *J. Biol. Chem.* **271,** 18237–18242 (1996).
16. Song, X. *et al.* A model for the quaternary structure of the proteasome activator PA28. *J. Biol. Chem.* **271,** 26410–26417 (1996).
17. Ma, C.-P., Willy, P. J., Slaughter, C. A. & DeMartino, G. N. PA28, an activator of the 20S proteasome, is inactivated by proteolytic modification at its carboxyl terminus. *J. Biol. Chem.* **268,** 22514–22519 (1993).
18. Löwe, J. *et al.* Crystal structure of the 20S proteasome from the archaeon *T. acidophilum* at 3.4 Å resolution. *Science* **268,** 533–539 (1995).
19. Groll, M. *et al.* Structure of 20S proteasome from yeast at 2.4 Å resolution. *Nature* **386,** 463–471 (1997).
20. Wenzel, T. & Baumeister, W. Conformational constraints in protein degradation by the 20S proteasome. *Nature Struct. Biol.* **2,** 199–204 (1995).
21. Hochstrasser, M. Ubiquitin, proteasomes, and the regulation of intracellular protein degradation. *Curr. Opin. Cell. Biol.* **7,** 215–223 (1995).
22. Jentsch, S. & Schlenker, S. Selective protein degradation: a journey's end within the proteasome. *Cell* **82,** 881–884 (1995).
23. Realini, C., Rogers, S. W. & Rechsteiner, M. KEKE motifs: Proposed roles in protein-protein association and presentation of peptides by MHC class I receptors. *FEBS Lett.* **348,** 109–113 (1994).
24. Otwinowski, Z. in *Data Collecton and Processing* (eds Sawyer, L., Isaacs, N. & Bailey, S.) 56–62 (SERC Daresbury Laboratory, Warrington, UK, 1993).
25. CCP4. The CCP4 suite: programs for protein crystallography. *Acta Crystallogr. D* **50,** 760–763 (1994).
26. Kleywegt, G. J. & Jones, T. A. in *From First Map to Final Model* (eds Bailey, S., Hubbard, R. & Waller, D.) 59–66 (SERC Daresbury Laboratory, Warrington, UK, 1994).
27. Jones, T. A., Zou, J.-Y., Cowan, S. W. & Kjeldgaard, M. Improved methods for building protein models in electron density maps and location of errors in these models. *Acta Crystallogr. A* **47,** 110–119 (1991).
28. Brünger, A. T. *X-PLOR Version 3.843, A System for X-ray Crystallography and NMR* (Yale University, New Haven, CT, 1996).
29. Laskowski, R. A., MacArthur, M. W., Moss, D. S. & Thornton, J. M. PROCHECK: a program to check the stereochemical quality of protein structures. *J. Appl. Crystallogr.* **26,** 283–291 (1993).
30. Kraulis, P. J. Molscript: a program to produce both detailed and schematic plots of protein structures. *J. Appl. Crystallogr.* **24,** 946–950 (1991).

Acknowledgements. We thank D. Worthylake and M. Mathews for assistance with data collection; V. Ramakrishnan, W. Sundquist, and members of C.P.H.'s and M.R.'s laboratories for critical comments on the manuscript. This work was supported by the American Cancer Society and the Lucille P. Markey Charitable Trust, S.C.J. was an NIH predoctoral trainee.

Correspondence and requests for materials should be addressed to C.P.H. (e-mail: chris@mssc.med.utah. edu). Coordinates (1avo) have been deposited in the Brookhaven Protein Data Bank.

correction

CTL induction by a tumour-associated antigen octapeptide derived from a murine lung carcinoma

Ofer Mandelboim, Gideon Berke, Mati Fridkin, Michael Feldman, Miriam Eisenstein & Lea Eisenbach

Nature **369,** 67–71 (1994)

In this Letter, we reported that the octapeptides Mut1 and 2 (52 FEQNTAQP and A59, respectively), thought to originate from a mutated form of the gap-junction protein connexin 37 with a Cys → Gln mutation in position 3 of the peptide, are shared tumour-specific antigenic epitope(s) of the C57BL/6 Lewis lung carcinoma 3LL clones D122 and K^b39.5, and that they are capable of inducing tumour-specific CTL, tumour immunoprotection, and immunotherapy of established lung metastasis (see also ref. 1). More recent experiments performed in the laboratory of one of us (G.B.) now call into question this finding and conclusions. The experimental details and results will be published elsewhere[2]; a preprint is available on request. □

1. Mandelboim, O. *et al.* Regression of established murine carcinoma metastases following vaccination with tumor associated antigen peptide. *Nature Med.* **1,** 1179–1183 (1995).
2. Rosen, D., Brookenthal, K. & Berke, G. An appraisal of the tumor immunoprotective and therapeutic activities of the octapeptides Mut1 and 2 from the mouse Lewis lung carcinoma 3LL. *J. Immunol.*, submitted.